Materials Chemistry and Physics 200 (2017) 354–360

Contents lists available at ScienceDirect

Materials Chemistry and Physics

journal homepage: www.elsevier.com/locate/matchemphys

Platinum nanoparticles supported on nitrogen-doped carbon for ammonia electro-oxidation

Vilmaria A. Ribeiro, Isabel C. de Freitas, Almir O. Neto, Estevam V. Spinacé, Júlio César M. Silva*

Instituto de Pesquisas Energéticas e Nucleares, IPEN/CNEN-SP, Av. Prof. Lineu Prestes, 2242 Cidade Universitária, CEP 05508-900, São Paulo, SP, Brazil

HIGHLIGHTS

- Nitrogen-doped carbon used as support for Pt nanoparticles (Pt/NC).
- The catalytic activity of Pt/NC for ammonia electro-oxidation.
- Superior catalytic activity of Pt/NC compared to Pt/C for ammonia electro-oxidation.

ARTICLE INFO

Article history:
Received 22 March 2017
Received in revised form
5 July 2017
Accepted 31 July 2017
Available online 1 August 2017

Keywords:
Platinum nanoparticles
Nitrogen-doped carbon
Ammonia electro-oxidation

ABSTRACT

Pt nanoparticles supported on carbon (Pt/C) and nitrogen-doped carbon (Pt/NC) were prepared by an alcohol-reduction process and used for ammonia electro-oxidation in alkaline media. Nitrogen-doped carbons were prepared by thermal treatment of urea and Carbon Vulcan XC72 at 800 °C under argon atmosphere. The obtained materials showed the presence of face centered cubic structure of Pt and mean particle sizes in the range of 3–3.7 nm. X-ray photoelectron spectroscopy results revealed that Pt/NC 5 (carbon prepared with 5% of urea) presents more Pt on the surface than Pt/C, and the nanoparticles are predominantly in the metallic state. The electrocatalytic activity was investigated by cyclic voltammetry and chronoamperometry experiments. Pt/NC materials showed a higher electrocatalytic activity for ammonia electro-oxidation than Pt/C, whereby the material Pt/NC 5 showed the peak current density 161% higher than Pt/C. The increase of activity might be related to the high electrochemically accessible area of Pt/NC and the improvement on the interaction with water due to the nitrogen onto the support which could contribute to the oxidation of intermediate products from ammonia electro-oxidation.

1. Introduction

Ammonia electro-oxidation has been attracting attention in the recently years from different prospects such as energy generation in the Direct ammonia fuel cells, production of high purity hydrogen and wastewater treatment [1,2]. Taking into account the environmental viewpoints, ammonia is a toxic pollutant in discharge water that leads to the eutrophication of the ecosystem [3–5]. Additionally, ammonia has been reported to be potentially harmful to public safety [5]. Thus, the study of ammonia electro-oxidation is an important issue in the energetic and environmental field [2,6].

Ammonia electro-oxidation is a slow process at low temperature and materials with high catalytic activity are required for this process [4]. Among various metals, platinum has been identified as the most effectively to promote ammonia electro-oxidation [1,4,7]. However, the catalytic activity of Pt towards ammonia electro-oxidation is affected by strongly adsorbed N_{ads} poisoning specie [4,7,8]. In order to overcome this issue, based platinum binary e.g. PtIr, PtPd, PtRu, PtRh, PtSn and PtAu [4,7,9–11] or multi-metallic electrocatalysts i.e. PtPdRh [5] are proposed in the literature.

The electrocatalysts for ammonia electro-oxidation are usually synthesized as nanoparticles and the most common support for the nanoparticles is carbon black due to its large surface area, high electrical conductivity, porous structures and low cost [12,13].

However, this inert material does not enhance electrocatalytic activities, but serves mostly as a mechanical support [12,14,15]. In order to improve the catalytic activity of the materials, different

* Corresponding author.
E-mail address: quimijulio@gmail.com (J.C.M. Silva).

http://dx.doi.org/10.1016/j.matchemphys.2017.07.088
0254-0584/

efforts have been devoted in the modification of carbon support [16,17]. In this sense, carbon has been doped with different elements, such as, N, B, S, Se [16]. Nitrogen-doped carbon black has been studied because nitrogen enhances electron-donor of the carbon material since nitrogen has one electron more than carbon in the external shell [16,17]. Thus, nitrogen-doped carbon materials have been used as a support to nanoparticles applied for different reactions such as glycerol electro-oxidation [18], methanol electro-oxidation [13], hydrogen evolution reactions [17] and oxygen reduction reaction [16,19]. In all these cases, the nitrogen-doped carbon has improved the electrocatalytic activity of the materials. According to the literature, nitrogen-doped carbon increases the support/catalyst chemical binding [13,18]. Synthesis of nitrogen-doped carbon can be carried out by two approaches, direct doping during the syntheses of the carbon materials or by post-doping treatment [13,16]. The post-doping approach consists in carbon treatment in the presence of a nitrogen source. Most part of the post-doping treatment are usually conducted at temperatures between 600 °C and 1100 °C depending on the precursor used [20]. Domínguez et al. [20] doped carbon nanotubes with nitrogen using urea as precursors, the process was carried out at thermal treatment at 800 °C.

To the best of our knowledge, there are no reports that study the effect of nitrogen-doped carbon used as a support to nanoparticles towards ammonia electro-oxidation. Thus, in the present study, carbon was doped with different percentages of urea, used as the source of nitrogen, and then used as support to platinum nanoparticles. The synthesized materials were evaluated towards ammonia electro-oxidation reaction.

2. Experimental

Nitrogen-doped carbons were prepared based on a procedure described in reference [21]. In this process, a physical mixture of urea (1, 2.5 and 5 wt%) and carbon Vulcan XC72 Cabot (previous treated at in a tubular oven at 800 °C under argon atmosphere) were heated (10 °C min^{-1}) under argon atmosphere in a tubular furnace at 800 °C and remained in this temperature for 1 h. After this, the obtained solids were washed with excess of water and dried at 70 °C for 2 h.

Platinum supported on carbon (Pt/C) and on Nitrogen-doped carbons (Pt/NC) electrocatalysts (20 wt% of Pt) were prepared by the alcohol-reduction process [21]. The Pt precursor, $H_2PtCl_6 \cdot 6H_2O$ (Sigma-Aldrich), was diluted in a solution containing 3 parts of ethylene glycol and 1 of water, then carbon (Vulcan XC72 Cabot) or N-doped carbons were added. The dispersions were kept in an ultrasonic bath for 20 min and submitted to reflux for 3 h under open atmosphere at 150 °C. Then, the resulting solids were filtered and washed with deionized water and dried in an oven at 70 °C for 2 h. In the end of this process, Pt nanoparticles supported on carbon denoted Pt/C, and Pt nanoparticles supported on Nitrogen-doped carbons prepared with 1%, 2.5% and 5 wt% of urea, denoted Pt/NC 1, Pt/NC 2.5 and Pt/NC 5, respectively, were obtained.

A Rigaku diffractometer model Miniflex II using Cu Kα radiation source (0.15406 nm) was used to characterize the synthesized materials by X-ray diffraction (XRD). The X-ray diffraction patterns were recorded with a step size of 0.05° and a scan time of 2 s per step from 2θ = 20°–90°.

A JEOL transmission electron microscope (TEM) model JEM-2100 operated at 200 kV was used to perform the analysis in order to obtain information about the distribution and sizes of the nanoparticles. About 200 nanoparticles at different regions of the materials were measured in order to construct the histograms.

The X-ray photoelectron spectroscopy (XPS) analysis were done with an SPECSLAB II (Phoibos-Hsa 3500 150, 9 channeltrons) SPECS spectrometer, with Al Kα source (E = 1486.6 eV) working at 15 kV, Epass = 40 eV, 0.2 eV energy step and 2 s per point was the acquisition time.

The synthesized materials were kept on stainless steel sample-holders and transported under inert atmosphere to the pre-chamber of the XPS staying there in a vacuum atmosphere for 2 h. The binding energies (BE) of Pt 4f, N 1s, O 1s and C 1s were referenced to the C 1s peak, at 284.5 eV, providing accuracy within ±0.2 eV.

Electrochemical measurements were performed with a potentiostat/galvanostat PGSTAT 302 N Autolab at room temperature and in a three-compartiment electrochemical cell made of Teflon. As counter electrode and reference electrode were used a platinum foil and a Hg/HgO, respectively. A Glassy carbon (GC) with the geometric area of 0.031 cm^2 was used as working electrodes to support the synthesized materials. Alumina (1 μm) was employed to polish the GC support before each experiment. In all experimental procedures Ultrapure water obtained from a Milli-Q system (Millipore®) was used.

The working electrodes were constructed by dispersing 6 mg of the electrocatalyst powder in 900 μL of water, 100 of μL isopropyl alcohol and 40 μL of 5% Nafion®. Then the mixture was dispersed in an ultrasonic bath for 30 min. Shortly thereafter, aliquots of 10 μL of the dispersion fluid were deposited onto the GC surface and dried for 20 min at 60 °C. 1 mol L^{-1} KOH solution was used in all the electrochemical measurements.

Cyclic voltammograms (CV) in ammonia free solutions were carried out at the potential range of −0.85 V to 0.1 V *vs* Hg/HgO at a scan rate of 20 mV s^{-1}. The electrocatalysts were cycled for five consecutive cycles resulting in the reproducible shape of the CVs. The CV in ammonia in the 1 mol L^{-1} KOH and 0.5 mol L^{-1} NH_4OH solution were carried out at a scan rate of 20 mV s^{-1} between −0.98 V and 0.2 V *vs* Hg/HgO. The electrocatalysts were cycled for three consecutive cycles and the third cycle is shown. Chronoamperometric experiments were carried out at − 0.30 V *vs.* Hg/HgO for 2 h. The catalyst electrochemical active surface area (ECSA) was measured using the charge involved in the hydrogen desorption [12].

3. Results and discussion

Fig. 1 shows the XRD patterns of the synthesized electrocatalysts Pt/C, Pt/NC 1, Pt/NCN 2.5 and Pt/NC 5. In all XRD patterns, a broad peak at about 25° 2θ is due to the (022) reflection of the hexagonal

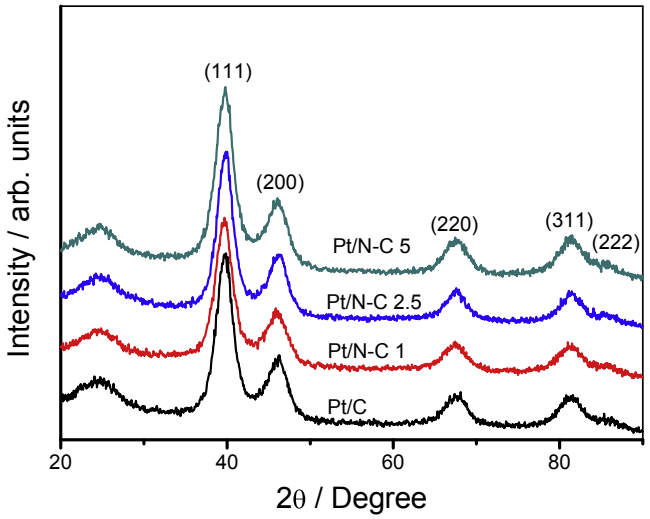

Fig. 1. X-ray diffraction patterns for Pt/C, Pt/C-N 1, Pt/C-N 2.5 and Pt/C-N 5 electrocatalysts.

structure of graphitic carbon [11,22]. The peaks at around 39, 46, 67, 81° 2θ are attributed to the face centered cubic (fcc) structure of Pt that correspond to (111), (200), (220) and (311) crystal planes, respectively [10,11]. The crystallite size, estimated using Scherrer equation and (220) peak [4,23] are 3.1, 3.7, 3.3 and 3.4 nm for Pt/CN 5, Pt/CN 2.5, Pt/CN 1 and Pt/C, respectively, and are in agreement with our previous work [24]. As it can be seen, the mean crystalline sizes of platinum are similar in the different materials.

The TEM micrographs and histogram of the particles sizes are shown in Fig. 2. As it can be seen, the platinum nanoparticles are

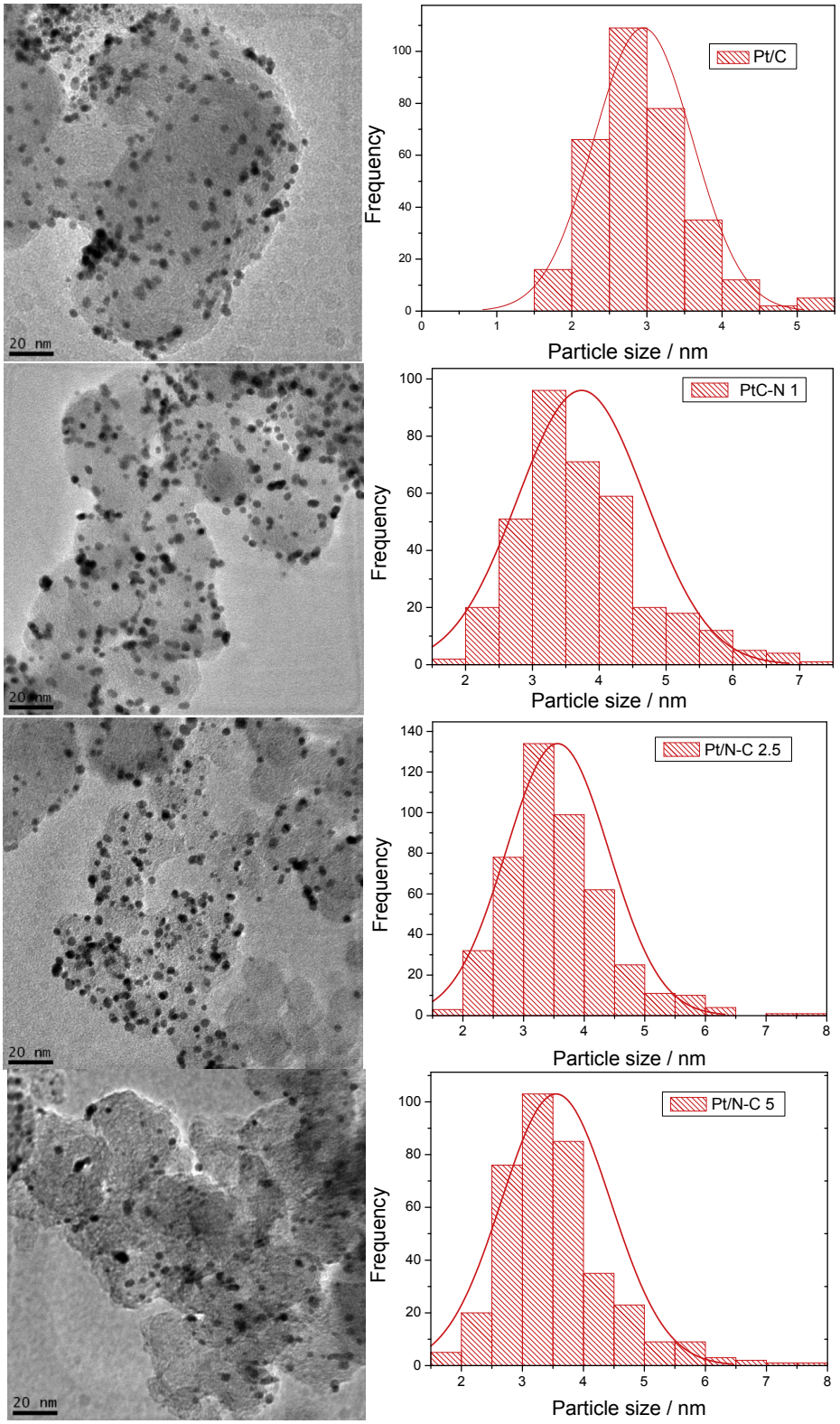

Fig. 2. TEM micrographs of Pt/C, Pt/N-C1, Pt/N-C 2.5 and Pt/N-C 5 electrocatalysts and their respective histograms.

well dispersed on the carbon support and smaller than 8 nm in all the cases which is characteristic of the alcohol reduction process [24,25]. The mean nanoparticle sizes of the platinum are 3.5 ± 0.9, 3.6 ± 0.9, 3.7 ± 0.9 and 3.0 ± 0.7, for Pt/CN 5, Pt/CN 2.5, Pt/CN 1 and Pt/C, respectively, are in agreement to our previous publication [26]. From the TEM analysis it is possible to see that the particles sizes are similar in all the materials.

To obtain information of the bonding state of the catalysts, XPS C 1s, O1s and Pt 4f core level spectra were recorded. As it can be seen in Fig. 3a, the C 1s spectrum was deconvoluted into six peaks [27]. The dominant peak at about 284.4 eV is assigned to graphitic carbon phase, whereas the peak at around 286 eV is related to hydrocarbons (C–H) from defects in the graphitic structure [27–29]. As it can be seen in Table 1, there were observed three more peaks which corresponds to carbon–oxygen bonding structures (–C–OH, >C=O and –COOH), and a peak assigned to π → π* plasmon excitation [27,29].

In Fig. 3b, the fitted O1s XPS spectra are shown. It was observed three peaks related to surface oxygen species at about 530, 533 and 535 eV assigned to surface oxygen species, which correspond to the lattice oxygen (O_L), surface oxygen species bonded to metal atoms or carbon support (O_S) and oxygen atoms bonded to carbon by double bonds (O_C) [27]. From Table 2, it is possible to see that the value of atomic XPS O 1s/C 1s ratio of Pt/C is lower than Pt/NC 5 (0.21 and 0.13, respectively), which indicates that Pt/C presents more oxygen on the surface than Pt/NC 5.

As shown in Fig. 3c, the deconvoluted Pt 4f spectrum are formed by three spin-orbit doublets with binding energies of Pt $4f_{7/2}$ components at ~71.4 eV, 72.6 eV and 74.4 eV, attributed to metallic Pt, $Pt(OH)_2$ and PtO_2 phases, respectively [10,30]. As the mean particle size is smaller than the XPS sampling depth (~5 nm) the XPS data reflect the core-shell structure of the catalyst, with a near surface region formed by external layers of PtO_2 and $Pt(OH)_2$ [10]. Taking into account the fitted peak areas of the Pt/C the hydroxide layers and oxides layers correspond to 37% of the peak area, while for Pt/NC 5 hydroxide layers and oxides layers correspond to 33% of the peak area. As it can be observed in Table 2, Pt/NC 5 presents higher percentage of Pt^0 than Pt/C. It is important to stress that the value of atomic XPS Pt 4f/C 1s ratio is higher for Pt/NC 5 than Pt/C (0.30 and 0.41, respectively) indicating that Pt/NC 5 presents more platinum on the surface that Pt/C.

From Fig. 3d it is possible to observe that the peak related to N 1s at around 400 eV [20]. Although it is possible to observe a peak related to nitrogen element spectra region for both CN 5 and Pt/NC

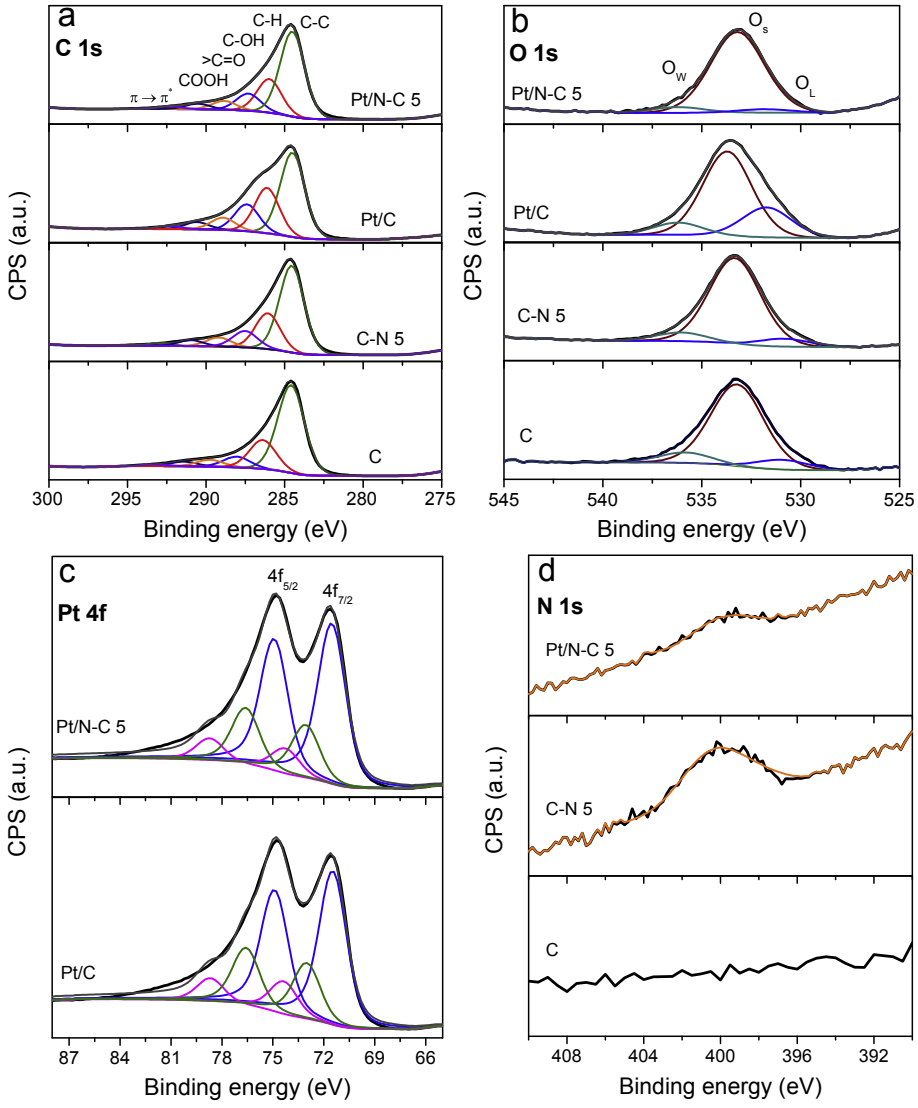

Fig. 3. Fitted XPS C 1s (a), O 1s (b) Pt 4f (c) and N 1s (d) of Pt/C, Pt/N-C 5, C and C-N 5.

Table 1
XPS characteristics of C 1s region for samples.

Sample	Binding energy (eV)					
	Peak I C–C	Peak II C–H (defects)	Peak III –C–OH	Peak IV > C=O	Peak V – COOH	Peak VI $\pi \rightarrow \pi^*$[a]
C	284.5 (61)[a]	286.4 (20)	288.0 (8)	289.6 (5)	290.7 (4)	293.2 (2)
CN 5	284.5 (55)	286.1 (23)	287.5 (10)	289.2 (6)	290.1 (4)	292.9 (2)
Pt/C	284.5 (47)	286.1 (25)	287.4 (15)	289.0 (7)	290.5 (4)	292.3 (2)
Pt/NC 5	284.5 (56)	286.0 (22)	287.3 (10)	288.9 (6)	290.5 (4)	292.3 (2)

[a] Percent of species.

Table 2
XPS characteristics of Pt 4f and O 1s region for samples.

Samples	Binding energy (eV)			Binding energy (eV)			Pt 4f/C 1s	O 1s/C 1s
	Pt (0)	Pt (II)	Pt (IV)	O_L	O_S	O_W		
C	n.d.	n.d.	n.d.	530.9 (10)	533.2 (80)	535.8 (10)	n.d.	0.06
CN 5	n.d.	n.d.	n.d.	530.8 (8)	533.3 (84)	536.0 (8)	n.d.	0.10
Pt/C	71,4 (63)[a]	72,6 (23)	74,4 (14)	531.7 (24)	533.7 (67)	536.2 (9)	0.30	0.21
Pt/NC 5	71,4 (67)	72,7 (22)	74,6 (11)	531,8 (4)	533.2 (90)	536.2 (6)	0.41	0.13

[a] Percent of species.

5, which was not seen for Pt/C, the presence of N on the surface are only in very small amount and the deconvolution of peaks was not performed because of noisy N 1s spectra. However, it is clear that the N is present in the carbon doped with urea.

The cyclic voltammetry of the electrocatalysts in 1 mol L^{-1} KOH in the potential range of −0.85 V to 0.1 V are shown in Fig. 4. As it can be observed, the shape of the CVs get broader as the amount of nitrogen-doping on the carbon support increases. These results suggest that Pt/NC 5 has the highest electrochemically accessible area. Curiously, the mean particles sizes obtained by TEM micrographs and by Scherrer equation from XRD are similar for all materials. This means that somehow the nitrogen on the support increases the platinum nanoparticles accessible area. In fact, from the XPS analysis was observed that Pt/NC 5 has more platinum on the catalyst surface than Pt/C, which explains the results from CV in 1 mol L^{-1} KOH.

The hydrogen adsorption/desorption process at about −0.73 V and −0.53 V are present on CVs [10,31]. The potential region from −0.30 to 0.1 V is associated with the formation of an oxide layer on the platinum surface [10,32] and the cathodic peak at around − 0.25 V is due to platinum oxide reduction [10,33].

In Fig. 5, it can be seen the CVs of the electrocatalysts in 1 M KOH +0.5 M NH_4OH. The shape of the CVs is in agreement to the reported in the literature for ammonia electro-oxidation on Pt/C [4,7,10,11]. As it can be observed, the onset potential for ammonia electro-oxidation shifts to lower potential as the amount of urea on carbon increases. The peak current density from ammonia electro-oxidation on Pt/NC 5 is about 56%, 95% and 161% higher than on Pt/NC 2.5, Pt/NC 1 and Pt/C, respectively. Thus, the highest catalytic activity of the Pt/NC 5 material is notable.

Pt/NC has also shown a higher catalytic activity than Pt/C towards methanol electro-oxidation [13]. Thamer et al. [34] performed experiments related to the methanol electro-oxidation on Ni nanoparticles supported on nitrogen-doped carbon nanofibers, and according to the authors the catalytic activity of the materials increased from 1% up to 4% of the N precursor. The improvement in the catalytic activity of the materials was attributed to an increase of the electronic conductivity of the carbon nanofibers by nitrogen and also an improvement of the wettability of the materials. Thus, the nitrogen doping carbon might improve the catalytic activity of platinum nanoparticles by different effects: (I) The electrochemically accessible area, since electrochemical active surface area

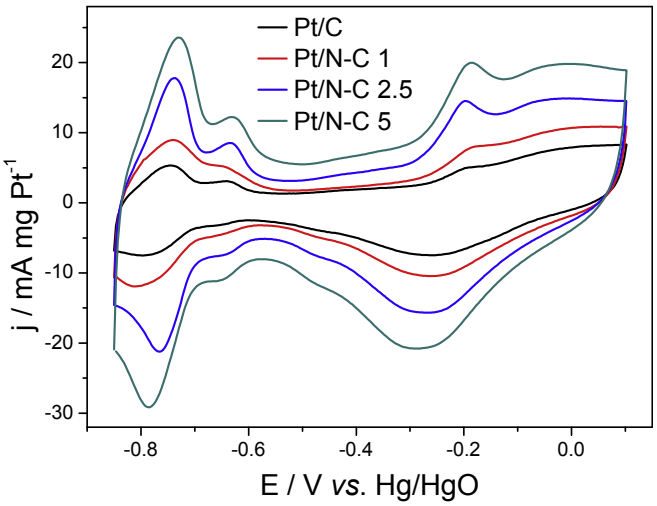

Fig. 4. Voltammograms of Pt/C, Pt/N-C 1, Pt/N-C 2.5 and Pt/N-C 5 in 1 moL L^{-1} KOH at 20 mVs^{-1}.

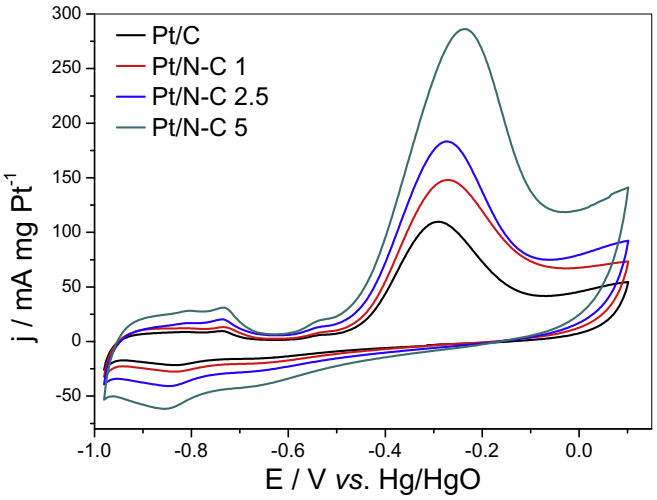

Fig. 5. Voltammograms of Pt/C, Pt/N-C 1, Pt/N-C 2.5 and Pt/N-C 5 in 1 moL L^{-1} KOH +0.5 moL L^{-1} NH_4OH at 20 mVs^{-1}.

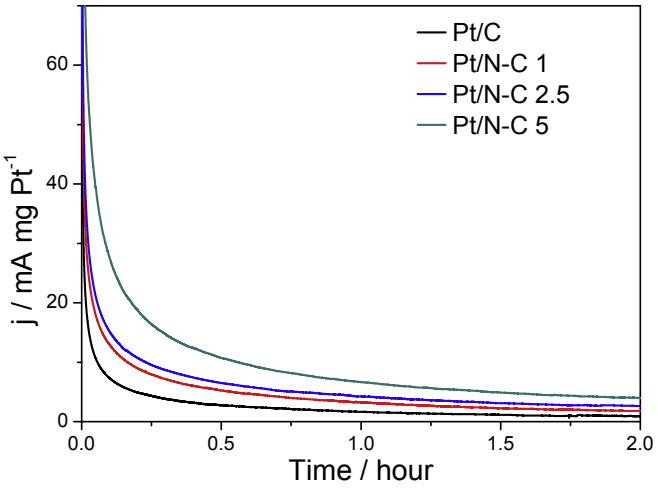

Fig. 6. Chronoamperometric results at − 0.35 V for Pt/C, Pt/N-C 1, Pt/N-C 2.5 and Pt/N-C 5 in 1 moL L^{-1} KOH +0.5 moL L^{-1} NH_4OH.

measured using the charge involved in the hydrogen desorption region was 4.2, 3.6, 2.4, and 1.1 cm^{-2}, for Pt/NC 5, Pt/N-C 2.5, Pt/NC 1 and Pt/C, respectively. (II) The improvement in the interaction with water due to the nitrogen onto the support, which could contribute to the oxidation of intermediates products from ammonia electro-oxidation [12].

In Fig. 6 are the results of chronoamperometry experiments at − 0.35 V during 2 h in the 1 mol L^{-1} KOH +0.5 mol L^{-1} NH_4OH. As it can be seen, the current density decreases significantly within the first minutes but becomes less pronounced after 30 min. The current continuous decline might be due to the surface poisoning by the inactive intermediates, i.e., N_{ads} as it was also reported in the literature for various Pt-based catalysts [4,10,35].

Similar to CV experiments, Pt/NC 5 has the highest current density compared to other electrocatalysts, whereas the current density on Pt/C was the lowest. Using Pt/NC 5 the current density from ammonia electro-oxidation was about 45%, 128% and 400% higher than using Pt/NC 2.5, Pt/NC 1% and Pt/C, respectively.

As it can be observed, in both CV and CA experiments, nitrogen doping carbon improves the catalytic activity of platinum towards ammonia electro-oxidation. These results are important since there are many reports in the literature in which binary or ternary electrocatalysts are proposed in order to improve the ammonia electro-oxidation reaction [4,7,9–11,36,37]. However, as the best of our knowledge, there are no studies using nitrogen-doping carbon as a support to platinum nanoparticles for ammonia electro-oxidation reaction.

4. Conclusions

The results of this work show that the ammonia electro-oxidation on platinum nanoparticles can be improved by nitrogen-doped carbon. As it was shown by TEM analysis, the mean particles sizes were from 3 to 3.7 nm for all the electrocatalysts synthesized and the nanoparticles were well dispersed on carbon and nitrogen-doped carbon support. According to XPS measurements, Pt/NC 5 presents more Pt and less oxygen on the surface than the Pt/C. In CA analysis, the current density from ammonia electro-oxidation at a 2-h experiment on Pt/NC 5 was about 400% higher than on Pt/C. It was also observed that the catalytic activity of the materials for ammonia electro-oxidation increases as the amount of urea used as a source of nitrogen to prepare nitrogen-doped carbon increases from 1 to 5%.

The improved catalytic activity might be related to the high electrochemically accessible area of Pt/NC materials and the enhancement of the interaction with water due to the nitrogen onto the support, which could contribute to the oxidation of intermediate products from ammonia electro-oxidation.

Acknowledgements

The authors wish to thank CNPq (Proc. No 166089/2015-0, 402850/2015-7, 168251/2014-0 and 310051/2012-6), FAPESP (Proc. No 2014/09087-4) and CAPES for the financial support, CCTM from IPEN-CNEN/SP for TEM measurements and Dr. Daniela Coelho de Oliveira for XPS experiments.

References

[1] J. Liu, B. Liu, Z. Ni, Y. Deng, C. Zhong, W. Hu, Improved catalytic performance of Pt/TiO2 nanotubes electrode for ammonia oxidation under UV-light illumination, Electrochim. Acta 150 (2014) 146–150.
[2] C. Zhong, W.B. Hu, Y.F. Cheng, Recent advances in electrocatalysts for electro-oxidation of ammonia, J. Mater. Chem. A 1 (2013) 3216–3238.
[3] A. Allagui, S. Sarfraz, S. Ntais, F. Al momani, E.A. Baranova, Electrochemical behavior of ammonia on Ni98Pd2 nano-structured catalyst, Int. J. Hydrogen Energy 39 (2014) 41–48.
[4] T.L. Lomocso, E.A. Baranova, Electrochemical oxidation of ammonia on carbon-supported bi-metallic PtM (M=Ir, Pd, SnOx) nanoparticles, Electrochim. Acta 56 (2011) 8551–8558.
[5] C.-M. Hung, Electrochemical properties of PtPdRh alloy catalysts for ammonia electrocatalytic oxidation, Int. J. Hydrogen Energy 37 (2012) 13815–13821.
[6] B.K. Boggs, G.G. Botte, Optimization of Pt–Ir on carbon fiber paper for the electro-oxidation of ammonia in alkaline media, Electrochim. Acta 55 (2010) 5287–5293.
[7] F.J. Vidal-Iglesias, J. Solla-Gullón, V. Montiel, J.M. Feliu, A. Aldaz, Screening of electrocatalysts for direct ammonia fuel cell: ammonia oxidation on PtMe (Me: Ir, Rh, Pd, Ru) and preferentially oriented Pt(1 0 0) nanoparticles, J. Power Sources 171 (2007) 448–456.
[8] A.C.A. de Vooys, M.T.M. Koper, R.A. van Santen, J.A.R. van Veen, The role of adsorbates in the electrochemical oxidation of ammonia on noble and transition metal electrodes, J. Electroanal. Chem. 506 (2001) 127–137.
[9] A. Allagui, M. Oudah, X. Tuaev, S. Ntais, F. Almomani, E.A. Baranova, Ammonia electro-oxidation on alloyed PtIr nanoparticles of well-defined size, Int. J. Hydrogen Energy 38 (2013) 2455–2463.
[10] M.H.M.T. Assumpção, R.M. Piasentin, P. Hammer, R.F.B. De Souza, G.S. Buzzo, M.C. Santos, E.V. Spinacé, A.O. Neto, J.C.M. Silva, Oxidation of ammonia using PtRh/C electrocatalysts: fuel cell and electrochemical evaluation, Appl. Catal. B Environ. 174–175 (2015) 136–144.
[11] J.C.M. Silva, S.G. da Silva, R.F.B. De Souza, G.S. Buzzo, E.V. Spinacé, A.O. Neto, M.H.M.T. Assumpção, PtAu/C electrocatalysts as anodes for direct ammonia fuel cell, Appl. Catal. A General 490 (2015) 133–138.
[12] J.C.M. Silva, R.M. Piasentin, E.V. Spinacé, A.O. Neto, E.A. Baranova, The effect of antimony-tin and indium-tin oxide supports on the catalytic activity of Pt nanoparticles for ammonia electro-oxidation, Mater. Chem. Phys. 180 (2016) 97–103.
[13] E. Antolini, Nitrogen-doped carbons by sustainable N- and C-containing natural resources as nonprecious catalysts and catalyst supports for low temperature fuel cells, Renew. Sustain. Energy Rev. 58 (2016) 34–51.
[14] K.-S. Lee, I.-S. Park, Y.-H. Cho, D.-S. Jung, N. Jung, H.-Y. Park, Y.-E. Sung, Electrocatalytic activity and stability of Pt supported on Sb-doped SnO2 nanoparticles for direct alcohol fuel cells, J. Catal. 258 (2008) 143–152.
[15] K.-W. Park, Y.-E. Sung, S. Han, Y. Yun, T. Hyeon, Origin of the enhanced catalytic activity of carbon nanocoil-supported PtRu alloy electrocatalysts, J. Phys. Chem. B 108 (2004) 939–944.
[16] N. Daems, X. Sheng, I.F.J. Vankelecom, P.P. Pescarmona, Metal-free doped carbon materials as electrocatalysts for the oxygen reduction reaction, J. Mater. Chem. A 2 (2014) 4085–4110.
[17] M. Zhang, S. Wang, T. Li, J. Chen, H. Zhu, M. Du, Nitrogen and gold nanoparticles co-doped carbon nanofiber hierarchical structures for efficient hydrogen evolution reactions, Electrochim. Acta 208 (2016) 1–9.
[18] M. Zhang, J. Shi, Y. Sun, W. Ning, Z. Hou, Selective oxidation of glycerol over nitrogen-doped carbon nanotubes supported platinum catalyst in base-free solution, Catal. Commun. 70 (2015) 72–76.
[19] Y. Hua, T. Jiang, K. Wang, M. Wu, S. Song, Y. Wang, P. Tsiakaras, Efficient Pt-free electrocatalyst for oxygen reduction reaction: highly ordered mesoporous N and S co-doped carbon with saccharin as single-source molecular precursor, Appl. Catal. B Environ. 194 (2016) 202–208.
[20] C. Domínguez, F.J. Pérez-Alonso, S.A. Al-Thabaiti, S.N. Basahel, A.Y. Obaid, A.O. Alyoubi, J.L. Gómez de la Fuente, S. Rojas, Effect of N and S co-doping of multiwalled carbon nanotubes for the oxygen reduction, Electrochim. Acta 157 (2015) 158–165.

[21] O.S.G.P. Soares, R.P. Rocha, A.G. Gonçalves, J.L. Figueiredo, J.J.M. Órfão, M.F.R. Pereira, Easy method to prepare N-doped carbon nanotubes by ball milling, Carbon 91 (2015) 114–121.
[22] M.H.M.T. Assumpção, S.G. da Silva, R.F.B. de Souza, G.S. Buzzo, E.V. Spinacé, A.O. Neto, J.C.M. Silva, Direct ammonia fuel cell performance using PtIr/C as anode electrocatalysts, Int. J. Hydrogen Energy 39 (2014) 5148–5152.
[23] J.C.M. Silva, B. Anea, R.F.B. De Souza, M.H.M.T. Assumpcao, M.L. Calegaro, A.O. Neto, M.C. Santos, Ethanol oxidation reaction on IrPtSn/C electrocatalysts with low Pt content, J. Braz. Chem. Soc. 24 (2013) 1553–1560.
[24] R.M. Antoniassi, A. Oliveira Neto, M. Linardi, E.V. Spinacé, The effect of acetaldehyde and acetic acid on the direct ethanol fuel cell performance using PtSnO2/C electrocatalysts, Int. J. Hydrogen Energy 38 (2013) 12069–12077.
[25] E.V. Spinacé, A.O. Neto, T.R.R. Vasconcelos, M. Linardi, Electro-oxidation of ethanol using PtRu/C electrocatalysts prepared by alcohol-reduction process, J. Power Sources 137 (2004) 17–23.
[26] A. Oliveira Neto, M. Brandalise, R.R. Dias, J.M.S. Ayoub, A.C. Silva, J.C. Penteado, M. Linardi, E.V. Spinacé, The performance of Pt nanoparticles supported on Sb2O5.SnO2, on carbon and on physical mixtures of Sb2O5.SnO2 and carbon for ethanol electro-oxidation, Int. J. Hydrogen Energy 35 (2010) 9177–9181.
[27] L. Zhang, F. Li, Helical nanocoiled and microcoiled carbon fibers as effective catalyst supports for electrooxidation of methanol, Electrochim. Acta 55 (2010) 6695–6702.
[28] M.H.M.T. Assumpção, A. Moraes, R.F.B. De Souza, R.M. Reis, R.S. Rocha, I. Gaubeur, M.L. Calegaro, P. Hammer, M.R.V. Lanza, M.C. Santos, Degradation of dipyrone via advanced oxidation processes using a cerium nanostructured electrocatalyst material, Appl. Catal. A General 462–463 (2013) 256–261.
[29] F.V.E. dos Reis, V.S. Antonin, P. Hammer, M.C. Santos, P.H.C. Camargo, Carbon-supported TiO2–Au hybrids as catalysts for the electrogeneration of hydrogen peroxide: investigating the effect of TiO2 shape, J. Catal. 326 (2015) 100–106.
[30] M. Ali, A. Witkowska, M. Abbas, R. Gunnella, A. Di Cicco, Evolution of the nanostructure of Pt and Pt–Co polymer electrolyte membrane fuel cell electrocatalysts at successive degradation stages probed by X-ray photoemission, J. Power Sources 271 (2014) 548–555.
[31] A. Santasalo-Aarnio, S. Tuomi, K. Jalkanen, K. Kontturi, T. Kallio, The correlation of electrochemical and fuel cell results for alcohol oxidation in acidic and alkaline media, Electrochim. Acta 87 (2013) 730–738.
[32] L. Jiang, A. Hsu, D. Chu, R. Chen, Ethanol electro-oxidation on Pt/C and PtSn/C catalysts in alkaline and acid solutions, Int. J. Hydrogen Energy 35 (2010) 365–372.
[33] L. Ma, D. Chu, R. Chen, Comparison of ethanol electro-oxidation on Pt/C and Pd/C catalysts in alkaline media, Int. J. Hydrogen Energy 37 (2012) 11185–11194.
[34] B.M. Thamer, M.H. El-Newehy, N.A.M. Barakat, M.A. Abdelkareem, S.S. Al-Deyab, H.Y. Kim, Influence of nitrogen doping on the catalytic activity of Ni-incorporated carbon nanofibers for alkaline direct methanol fuel cells, Electrochim. Acta 142 (2014) 228–239.
[35] M.H.M.T. Assumpção, S.G. da Silva, R.F.B. De Souza, G.S. Buzzo, E.V. Spinacé, M.C. Santos, A.O. Neto, J.C.M. Silva, Investigation of PdIr/C electrocatalysts as anode on the performance of direct ammonia fuel cell, J. Power Sources 268 (2014) 129–136.
[36] K. Endo, K. Nakamura, Y. Katayama, T. Miura, Pt–Me (Me = Ir, Ru, Ni) binary alloys as an ammonia oxidation anode, Electrochim. Acta 49 (2004) 2503–2509.
[37] H. Kim, D. Won, H.-K. Lee, S.J. Yoo, K.S. Nahm, P. Kim, Effect of the type of Pt precursor on Pt–Ni nanostructures for electro-oxidation of ammonia, Mater. Chem. Phys. 147 (2014) 722–727.